Biogeography **17.**
61–85. Sep. 20, 2015

Genetic isolation of the mottled spinefoot *Siganus fuscescens* Ryukyu Archipelago population

Kensuke Iwamoto[1, #], Muhamad Fadry Abdullah[1], Chih-Wei Chang[2], Tetsuo Yoshino [3] and Hideyuki Imai [1]*

[1] Laboratry of Marine Biology and Coral Reef Studies, Faculty of Science, University of the Ryukyus, Nishihara, Okinawa 903-0213, Japan
[2] National Museum of Marine Biology and Aquarium, and Graduate Institute of Marine Biology, National Dong Hwa University, Checheng, Pingtung 944, Taiwan, R.O.C.
[3] General Research Center, Okinawa Churashima Foundation, Ishikawa, Motobucho, Okinawa 905-0206, Japan

Abstract. A nucleotide sequence analysis of the mitochondrial DNA control region was conducted to reveal the genetic population structure and demographic history of the mottled spinefoot *Siganus fuscescens* (Houttuyn, 1782), and we discussed the taxonomic treatment of *S. fuscescens* and white-spotted spinefoot *S. canaliculatus* (Park, 1797) in terms of population genetics and morphological studies. Sequence analysis indicated that the haplotypes could be clearly divided into three lineages. Morphological analysis indicated no significant differences among measurements for the three genetically divergent lineages. We concluded that each lineage had once been isolated, and then former allopatric lineages may have resulted in the sympatric distribution of lineages due to secondary contact. *Siganus fuscescens* regards as valid species, and *S. canaliculatus* is a junior synonym of *S. fuscescens*.

Key words: genetic isolation, Ryukyu Archipelago, *Siganus fuscescens*

Introduction

The dispersal among populations in coastal fishes primarily occurs achieved during their pelagic larval phase, as most adult coastal fishes do not move far from their home. Dispersal may take place over large distances, particularly if larvae drift passively with the ocean currents (Roberts, 1997). The Kuroshio is a western boundary current that transports marine organisms long distances northwards rapidly. Senou *et al*.(2006), however, suggested that the Kuroshio plays an important role not only in transporting but also in forming a strong barrier against dispersal, and the Ryukyu Archipelago are relatively isolated by the Kuroshio barrier from the main islands of Japan, Taiwan and the Philippines since marine organisms are hard to cross this strong current (Aoki *et al.* 2008a; Aoki *et al.* 2008b; Imai and Aoki, 2012; Iwamoto *et al.* 2012; Imai *et al* 2013; Kuriiwa *et al*. 2014).

The mottled spinefoot *Siganus fuscescens* (Houttuyn, 1782) is a species of siganid with the greatest latitude range of that family. *Siganus fuscescens* lives in shallow water on the flats and lagoons of coral reefs throughout the Indo-West Pacific (Woodland, 1990). This is an economically important fish

#Present address: WDB Enrironmenntal & Reserch Institute CO. LTD., Yamagawauchi, Minami-cho, Tokushima 779-2307, Japan.

*Corresponding author: imai@sci.u-ryukyu.ac.jp

resource, and it is important to conserve this species against overfishing (Soliman *et al*. 2009). At the same time, *S. fuscescens* is regarded as harmful, because browsing by herbivorous fishes has recently caused seaweed/sea-grass bed reduction in warm temperate waters in the coastal areas of Japan (Fujita, 2006). With the rising seawater temperature due to global warming, these fish browse throughout the year, causing rocky-shore denudation (Hasegawa *et al*. 2003). Thus, we need to elucidate and understand the genetic structure and connectivity of siganids if we manage commercial aquatic resources and monitor the dynamics of the coastal environment.

The white-spotted spinefoot *S. canaliculatus* (Park, 1797) is also an herbivorous fish widely distributed in shallow waters throughout the Indo-West Pacific, and its range overlaps with that of *S. fuscescens* (Woodland, 1990). These species are morphologically very similar, and these sibling species have caused considerable taxonomic confusion (Woodland, 1990). The two species are usually morphologically identified based on the number of rows of spots between the first dorsal fin spine and the lateral line, and the head length to pectoral fin length ratio, as described in Woodland (1990) and Shimada (2000). *Siganus fuscescens* has four to six rows of spots and a head length to pectoral fin length ratio of 1.3–1.5, whereas *S. canaliculatus* has two to three rows of spots and a head length to pectoral fin length ratio of 1.1–1.3. The authors of previous studies, however, have been divided in their taxonomical opinions: Yamaoka *et al*. (1994), Kuriiwa *et al*. (2007) and Hsu *et al*. (2011a) have considered that what appears as two species is actually only color morphs within species (*i.e.*, synonyms), whereas Borsa *et al*. (2007) and Ravago-Gotanco *et al*. (2010) have suggested that these are distinct species.

In this study, we consider *S. canaliculatus* as a population of *S. fuscescens*, according to the description by Shimada (2000) and also sampled fish from type locality location of *S. canaliculatus*; Sumatra.

The objective of this study was to elucidate the genetic variability and population structure in *S. fuscescens* by mitochondrial DNA control region sequence analyses. We discuss the influence of the ocean currents and geographical situation on the genetic population structure and refer to the relationship between *S. fuscescens* and *S. canaliculatus* in terms of population genetics and morphological study.

Materials and Methods

Ethics statement

Fish in this study were purchased from local commercial fishers and fully complied with local fisheries management and marine protected area controls. Therefore, no specific permits were required for the described field sampling as the fishers were required to comply with local laws regarding capture. The species sampled are not endangered or protected.

Specimens

For genetic structure analysis based on mtDNA control region sequences, a total of 715 specimens were collected from around the main islands of Japan [Tateyama in Chiba Prefecture (CB, n = 47), Shimizu and Omaezaki in Shizuoka Prefecture (SZ, n = 56), Ohsumi in Kagoshima Prefecture (KG, n = 52)], the Ryukyu Archipelago [Amami Island in Kagoshima Prefecture (AM, n = 53), Okinawa Island (OK, n = 53), Miyako Island (MY, n = 54), and Ishigaki Island (IS, n = 45) in Okinawa Prefecture], Cheju Island in Korea (CJ, n = 36), Pingtung in Taiwan (TW, n = 49), the Philippines [Cebu Island (PH1, n = 42) and Tabaco (PH2, n = 30)], Songkhla in Thailand (TH, n = 27), Hai-Phong in Vietnam (VT, n = 49), Carp Island in Palau (PA, n = 20), Sorong in Indonesia (SR, n = 49), and the type locality location of *S. canaliculatus* which was Indian Ocean side of Sumatra Island in Indonesia (SM, n =

Table 1. Summary of *Siganus fuscescens* sample abbreviations, sampling localities, sample size (N), year and genetic diversity. SD, Standard deviation are in parentheses. Nh, number of haplotypes; ti, transition; tv, transversion; *h*, haplotype diversity; *k*, mean pairwise differences; π, nucleotide diversity

Localities	Abbr.	Geographic coordinate	N	Year	Nh	Substitutions [ti + tv]	Indels	*h* (SD)	*k* (SD)	π (SD)
Tateyama, Chiba, Japan	CB	34°58'N, 139°48'E	47	2010	15	35 [28 + 7]	5	0.709 (0.071)	3.520 (1.824)	0.008 (0.005)
Shimizu & Omaezaki, Shizuoka, Japan	SZ	34°37'N, 138°12'E	56	2008	25	32 [30 + 2]	4	0.784 (0.059)	4.320 (2.170)	0.010 (0.005)
Ohsumi, Kagoshima, Japan	KG	31°01'N, 130°40'E	52	2008	21	41 [33 + 8]	5	0.786 (0.060)	4.072 (2.064)	0.009 (0.005)
Cheju Island, Korea	CJ	33°30'N, 126°31E	36	2011	17	35 [29 + 6]	5	0.881 (0.047)	4.775 (2.389)	0.011 (0.006)
Amamioshima Is., Kagoshima, Japan	AM	28°22'N, 129°29'E	53	2009	20	27 [26 + 1]	3	0.918 (0.020)	8.025 (3.787)	0.018 (0.009)
Okinawajima Island, Okinawa, Japan	OK	26°19'N, 127°50'E	53	2007	19	27 [26 + 1]	3	0.898 (0.024)	7.811 (3.694)	0.018 (0.009)
Miyakojima Island, Okinawa, Japan	MY	24°48'N, 125°16'E	54	2008	21	27 [25 + 2]	3	0.867 (0.037)	7.769 (3.675)	0.017 (0.009)
Ishigakijima Island, Okinawa, Japan	IS	24°23'N, 124°11'E	45	2007	12	21 [20 + 1]	2	0.864 (0.034)	6.268 (3.031)	0.014 (0.008)
Pingtung, Taiwan	TW	22°02'N, 120°41'E	49	2007-2008	23	43 [36 + 7]	4	0.781 (0.064)	7.220 (3.442)	0.016 (0.009)
Cebu Island, Philippines	PH1	10°20'N, 123°51'E	42	2007	18	16 [16 + 0]	2	0.896 (0.034)	2.480 (1.367)	0.006 (0.003)
San Miguel, Tabaco, Philippines	PH2	13°21'N, 123°51'E	30	2010	13	11 [11 + 0]	2	0.938 (0.018)	3.143 (1.675)	0.007 (0.004)
Hai Phong, Vietnam	VT	20°48'N, 106°48'E	49	2011	27	42 [35 + 7]	5	0.874 (0.044)	9.862 (4.591)	0.022 (0.011)
Songkhla, Thailand	TH	7°12'N, 100°35'E	27	2009	17	39 [30 + 9]	3	0.926 (0.039)	9.444 (4.474)	0.021 (0.011)
Sibolga, Sumatra, Indonesia	SM	0°57'S, 100°21'E	53	2009	31	51 [43 + 8]	4	0.921 (0.027)	9.054 (4.234)	0.020 (0.011)
Carp Island, Palau	PA	7°5'N, 134°16'E	20	1999-2005	13	16 [16 + 0]	2	0.911 (0.054)	2.474 (1.394)	0.006 (0.003)
Sorong, West Papua, Indonesia	SR	0°52'S, 131°14'E	49	2012	15	28 [25 + 3]	5	0.872 (0.027)	5.231 (2.574)	0.012 (0.006)

53) between 2007 and 2012 (Table 1; Fig. 1).

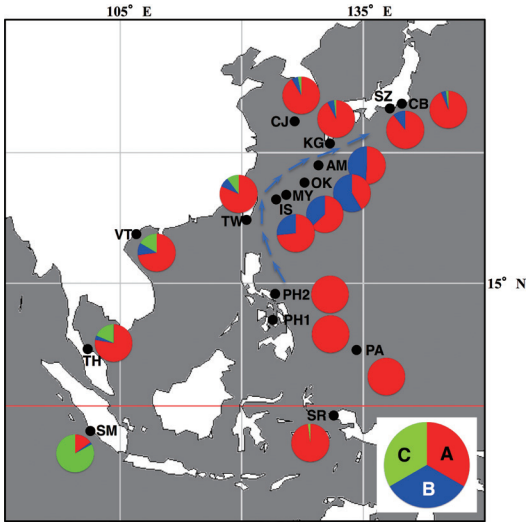

Fig. 1. Sampling locations for *Siganus fuscescens* and clades frequencies. Frequencies of individuals belonging to three phylogenetic clades of *Siganus fuscescens* from 16 localities . The Kuroshio current is shown with solid arrows.

Molecular methods

Total genomic DNA was extracted from approximately 50 mg of fresh, frozen, or ethanol-preserved muscle tissue or fin clip using the proteinase K, phenol-chloroform procedures with TNES-8M urea buffer (Imai *et al*. 2004).

The partial mitochondrial control region was amplified for population genetic analysis using forward primers L15926 (Kocher, 1989) or L15923 (Shields and Kocher, 1991) and H16498 (Meyer *et al*. 1990). Several samples showed no amplification products using these primers. Therefore, a new forward primer L-*Siganus*-Thr (5'-GCACTAGTAGCTCAGCTTCAGAGC-3') situated within the transfer RNA region ($tRNA^{Thr}$) gene was designed for siganid species based on the complete mitochondrial genome sequences of *Siganus fuscescens* (DNA Data Bank of Japan (DDBJ) Accession Number: EF025185) and *Siganus unimaculatus* (AP006031). Subse-

quently, the polymerase chain reaction (PCR) was performed with L-*Siganus*-Thr and H16498. PCR was performed using BIOTAQ™ DNA Polymerase (Bioline Ltd.), *Ex Taq*™ DNA polymerase (TaKaRa Bio, Inc.), or KAPA*Taq*™ EXtra DNA Polymerase (Kapa Biosystems). Each 50-µl aliquot of reaction mixture contained the following reagents with sterile distilled H_2O: For BIOTAQ™, 1 µl of template DNA, 12.5 pmol of each primer, 5 µl of 10×NH_4 reaction buffer, 5 µl of 10 mM deoxyribonucleotide triphosphate (dNTP) mixture, 4 µl of 50 mM $MgCl_2$ solution, and 2.5 units of Taq Polymerase; for *Ex Taq*™, 1 µl of template DNA, 12.5 pmol of each primer, 5 µl of 10×Ex *Taq*™ buffer, 5 µl of 2.5 mM dNTP mixture, and 2.5 units of *Taq* Polymerase; for KAPA*Taq*™, 1 µl of template DNA, 12.5 pmol of each primer, 10 µl of 5×KAPA*Taq* EXtra buffer, 1.5 µl of 10 mM dNTP mixture, 3.5 µl of 25 mM $MgCl_2$ solution, and 2.5 units of *Taq* Polymerase. The PCR conditions consisted of plate heating (94ºC, 2 min) and 30 cycles of denaturation (94ºC, 30 s), annealing (51–58ºC, 30 s), and extension (72ºC, 1 min), and a single final extension (72ºC, 7 min) using the thermal cycler GeneAmp 9700 (Applied Biosystems).

PCR products were purified using ExoSAP-IT (USB Co.) or a PCR Product Pre-Sequencing kit (USB Co.). Amplified DNA was sequenced on a CEQ 8800 automated DNA sequencer (Beckman Coulter) using the GenomeLab DTCS – Quick Start kit (Beckman Coulter) and on the ABI 3700 genetic analyzer (Applied Biosystems) with the Big Dye Terminator Cycle Sequencing kit ver. 3.1 (Applied Biosystems). Obtained sequence data were aligned using Clustal W (Thompson *et al.* 1997) and edited manually for each analysis. The sequences obtained in the present study were deposited in the DNA Data Bank of Japan (DDBJ) under Accession Numbers AB998923 to AB999078.

Population genetic structure analysis

The number of mtDNA haplotypes, haplotype diversity (*h*) (Nei, 1987), nucleotide diversity (π) (Tajima, 1983), and mean number of nucleotide pairwise differences (*k*) (Tajima, 1983) were calculated for each population using the computer software program ARLEQUIN version 3.5 (Excoffier and Lischer, 2010). To depict phylogenetic and geographical relationships of the haplotypic sequences with the number of individuals, we created a minimum-spanning tree (MST) using ARLEQUIN and then drew the results by hand. The MST of haplotypes was constructed under haplotype pairwise differences, showing the number of mutation steps between haplotypes. In addition, PAUP version 4.0 (Swofford, 2002) was employed for phylogenetic analysis of *S. fuscescens* haplotypes. Genetic distances were calculated using Kimura's two-parameter (K2P) model (Kimura, 1980), and a neighbor-joining tree (Saitou and Nei, 1987) was constructed based on the distance. To evaluate the robustness of the internal branches, 1,000 bootstrap replications (Felsenstein, 1985) were executed. The mtDNA control region sequence data of *S. spinus* obtained in this study was used as the outgroup.

Pairwise fixation indices (F_{ST}) and gene flow (*Nm*) between populations were estimated, and the significance of the *F* statics for population comparisons was assessed using 10,000 permutations. The genetic structure was examined by analysis of molecular variance (AMOVA) (Excoffier *et al*. 1992) in ARLEQUIN. Groups for AMOVA, defined according to pairwise F_{ST} dendrograms based on pairwise F_{ST} using the unweighted pair group method with arithmetic mean (UPGMA) (Sokal and Michener, 1958), were estimated using Phylip ver. 3.6 (Felsenstein, 2004). A pairwise mismatch distribution, comprised of the pairwise differences among all haplotypes, was performed for the historical demographic test. In addition, the Tajima's *D* (Tajima, 1989) and Fu's

Fs (Fu, 1997) tests were employed to find departures from mutation-drift equilibrium and to examine the demographic history. The neutrality test was applied to examine deviations of Tajima's *D* and Fu's F_S values from a neutral state. Furthermore, the population expansion parameters τ (time since expansion), θ_0, and θ_1 (the population size before and after expansion, respectively) and their probabilities were calculated in ARLEQUIN (Rogers and Harpending, 1992; Rogers, 1995). Tau (τ) can be used to estimate the time (T) since the population expansion as $T = \tau/2u$ and $u = 2\mu k$, where μ is the mutation rate for the entire DNA region under study and k is the length of the sequence (Rogers and Harpending, 1992; Harpending, 1994). The mutation rates of 4–10% MY^{-1} were used for the current study (Iwamoto *et al*. 2012).

To determine whether the extent of genetic differentiation was correlated with the geographic distance among populations, we performed a Mantel test with pairwise F_{ST} values and geographical distance between sampling locations over the entire study area in ARLEQUIN. This test was also carried out separately for the populations in the regions affected by the Kuroshio (*i.e*., CB, SZ, KG, CJ, AM, OK, MY, IS, TW, PH1, and PH2) to assess the influence of the Kuroshio on genetic connectivity in this species. Geographic distances were measured according to the shortest distance between the midpoints of sampling locations in km using the path tool in Google Earth 5.2 (available at http://earth.google.com). A pattern of isolation by distance (IBD) would be supported by a positive correlation between genetic differentiation and geographical distance. The test incorporated 10,000 permutations.

Morphological analysis

Thirty body dimensions were measured by digital caliper (to 0.1 mm) after fixation in 70% ethanol: (a) standard length; (b) body depth; (c) head length; (d) upper jaw length; (e) snout length; (f) orbit diameter; (g) suborbital length; (h) interorbital width; (i) predorsal length; (j_1) dorsal fin base length; (j_2) first dorsal spine length; (j_3) second dorsal spine length; (j_4) longest dorsal spine length; (j_5) last dorsal spine length; (j_6) longest dorsal ray length; (k) longest pectoral fin length; (l) prepelvic length; (m) longest pelvic fin length; (n) preanal length; (o_1) anal fin base length; (o_2) first anal spine length; (o_3) second anal spine length; (o_4) longest anal spine length; (o_5) last anal spine length; (o_6) longest anal ray length; (p) caudal peduncle length; (q) caudal peduncle width; (r_1) length of upper lobe of caudal fin; (r_2) middle caudal fin length; (r_3) length of lower lobe of caudal fin (Fig. 2). To assess differences in morphometric characteristics among genetically defined clades in the genetic analysis of the present population, we conducted a principle component analysis (PCA) on 30 characteristics using the PCA macro program with Microsoft Excel on the Windows platform (Fig. 2). We also plotted the relationship between head length and longest pectoral fin length to reconfirm the validity of the most common taxonomic key for identifying *S. fuscescens* and *S. canaliculatus* (see the Introduction). All morphometric characteristics were standardized by log transformation. Voucher specimens were deposited at the Okinawa Churaumi Fundation (formerly University of the Ryukyus) (Appendix 1).

Results

Genetic variability

A total of 449 base pair (bp) of the DNA segment containing the 45-bp partial $tRNA^{Thr}$ gene, entire 68-bp $tRNA^{Pro}$ gene, and partial mtDNA control region was determined from 715 specimens of *S. fuscescens* sampled from 16 localities. There were 77 polymorphic sites within the fragment, which defined 68 transitions, 15 transversions, and 6 indels.

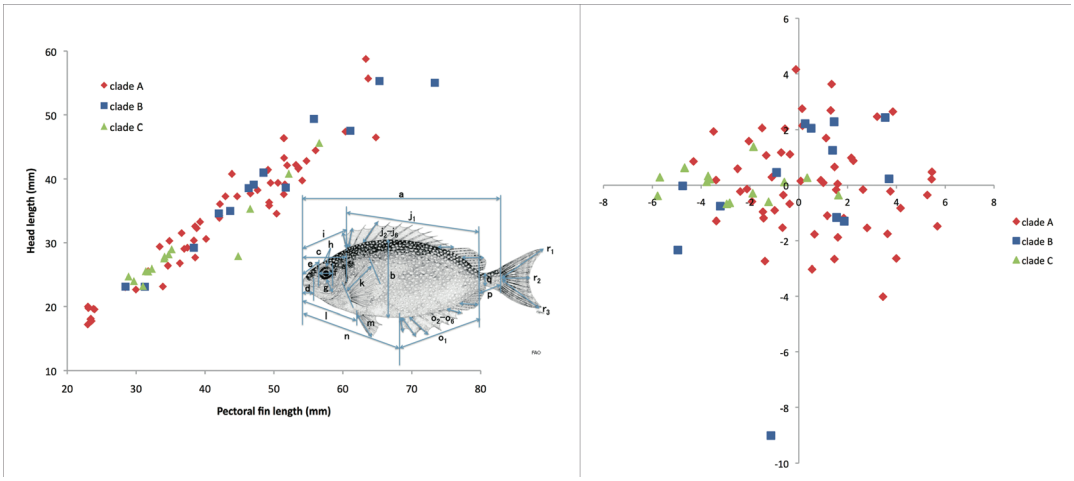

Fig. 2. Morphometric measurements of *Siganus fuscescens*. Diagram showing 30 body dimensions: (a) standard length; (b) body depth; (c) head length; (d) upper jaw length; (e) snout length; (f) orbit diameter; (g) suborbital length; (h) interorbital width; (i) predorsal length; (j_1) dorsal fin base length; (j_2) first dorsal spine length; (j_3) second dorsal spine length; (j_4) longest dorsal spine length; (j_5) last dorsal spine length; (j_6) longest dorsal ray length; (k) longest pectoral fin length; (l) prepelvic length; (m) longest pelvic fin length; (n) preanal length; (o_1) anal fin base length; (o_2) first anal spine length; (o_3) second anal spine length; (o_4) longest anal spine length; (o_5) last anal spine length; (o_6) longest anal ray length; (p) caudal peduncle length; (q) caudal peduncle width; (r_1) length of upper lobe of caudal fin; (r_2) middle caudal fin length; (r_3) length of lower lobe of caudal fin. Plot of head length vs. longest pectoral fin length of three clades of *Siganus fuscescens*. (left). Plots of the first two principal component (PC) scores based on 30 morphometric characteristics of three clades of *Siganus fuscescens* (right).

Of these 77 variable sites, 24 were phylogenetically informative. One hundred and fifty-six haplotypes (Sf1 to Sf156) were identified among 715 sampled individuals, 108 of which were unique or endemic to the sampling sites. Haplotype Sf1 was common to 144 sampled individuals (20.14%) and was shared among all sampling sites, with the exception of two Philippine populations (PH1 and PH2) and Sorong population (SR) (Appendix 2 and Fig. 3). Haplotype diversity indices for each population ranged from 0.709 (CB) to 0.938 (PH2). Nucleotide diversity varied among populations, ranging from 0.006 (PH1) to 0.022 (VT) (Table 1).

Genetic structure

The neighbor-joining tree of the haplotypes of *S. fuscescens* (Fig. 4), clearly indicated that the haplotypes of *S. fuscescens* are divided into three clades with high probabilities of bootstrapping. However, these clades did not appear to have a clear geographic structure, and there were no significant genealogical branches or clusters of samples corresponding to sampling locality. Although the nucleotide sequences among the three clades were clearly different (K2P distance 1.6–5.7%), the genetic distances were smaller than the inter-specific difference between *S. fuscescens* and one of the closest congeners in the family Siganidae, *S. spinus* (K2P distance 6.7–8.0%). The MST also indicated that the haplotypes could be divided into three clades (Fig. 3). Of the 715 sampled individuals, 535 belonged to clade A, 113 belonged to clade B, and 67 belonged to clade C. In the Ryukyu Archipelago (*i.e.*, AM, OK, MY, and IS), the percentage of individuals belonging to clade B was higher than that in other populations, and in the populations of the main island of Japan (*i.e.*, CB, SZ, and KG), Cheju Island (CJ) and Sorong Island (SR), most of the examined individuals belonged to

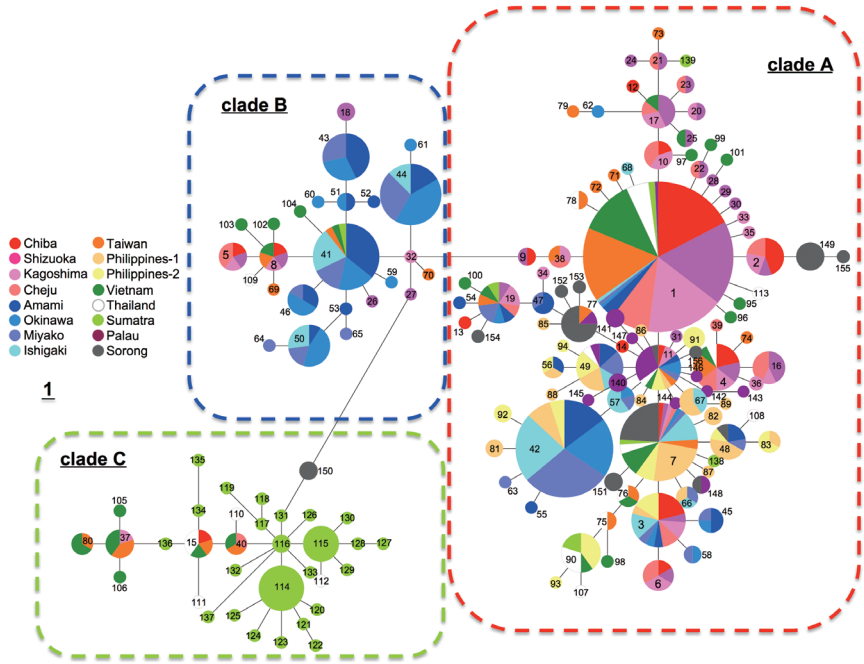

Fig. 3. Minimum spanning tree presenting relationships among 156 haplotypes of *Siganus fuscescens*. Numerals indicate haplotype numbers. The relative size of each circle represents the number of individuals. The scale bar indicates one substitution.

clade A (89–94%). The proportion of individuals belonging to clade C was larger toward the southwest, although no individuals belonging to clade C were found in the SZ, the two PH sites, the PA, or the Ryukyu Archipelago (Fig. 1).

The calculated pairwise F_{ST} values among populations are shown in Table 2. Most of the pairwise F_{ST} values between paired populations were highly significant ($P < 0.01$, 0.001) corroborated with the Bonferroni test [34]. The values did not significantly differ among groups of populations, as follows: CB, SZ, KG, and CJ ($F_{ST} = 0.000$, $P > 0.05$); TW, VT, and TH ($F_{ST} = 0.000$–0. 014, $P > 0.05$). Although the Ryukyu Archipelago lie between these regions, pairwise comparisons of F_{ST} indicated no significant genetic differentiations between populations of the main island of Japan (*i.e.*, CB, SZ, and KG) and CJ, and TW ($F_{ST} = 0.012$–0.020, $P > 0.05$), whereas F_{ST} values between the five populations and the Ryukyu Archipelago populations (*i.e.*, AM, OK, MY, and IS) were high, with highly significant differentiation ($F_{ST} = 0.107$–0.365, $P < 0.001$). In all comparisons of paired populations, the SM was obviously isolated alone, with extremely high pairwise F_{ST} and significant P values ($F_{ST} = 0.474$–0.700, $P < 0.001$). The estimated gene flow per generation (Nm) varied from 0.215 to infinite (Table 2). The pairing among the CB, SZ, KG, and CJ populations showed infinite Nm values, indicating that an extremely high level of gene flow has occurred between these populations over a large geographic distance. The Nm values between the VT and TW or TH populations were also very high. Similar to pairwise F_{ST} values, gene flow between populations of the main island of Japan and CJ, and TW ($Nm = 25.116$–41.523) was very high, whereas values between these five populations and the Ryukyu Archipelago populations were smaller ($Nm = 0.871$–4.172). In addition, Nm showed re-

stricted gene flow between the SM and the other populations (*Nm* = 0.215–0.556).

The unweighted pair group method with arithmetic means (UPGMA) dendrogram showed that populations from 16 localities were grouped into three clades, as follows: the first clade contained populations from the main island of Japan (CB, SZ, and KG), CJ, TW, PH1, PH2, VT, TH, PA, and SR, the second clade contained populations from the Ryukyu Archipelago (AM, OK, MY, and IS), and the third clade included the SM population (Fig. 5). AMOVA among three groups was performed on the basis of clades inferred from the UPGMA-based of pairwise F_{ST} values. A significant AMOVA test ($P < 0.001$) resulted in the proposed population subdivision into three groupings: (CB, SZ, KG, CJ, TW, PH1, PH2, VT, TH, PA, and SR), (AM, OK, MY, and IS), and (SM). Only 3% ($F_{SC} = 0.063$) of variance was ascribed to variation among populations within groups, whereas 39.20% ($F_{CT} = 0.392$) was ascribed to variation among groups, and 57.26% ($F_{ST} = 0.430$) to variation within populations (Table 3).

The Mantel test indicated a significant correlation ($r = 0.483$, $P < 0.05$) for geographic distance versus pairwise F_{ST} values over the entire study area, indicating isolation by distance. However, there was evidence of significant correlation for the 11 localities in the regions affected by the Kuroshio (CB, SZ, KG, CJ, AM, OK, MY, IS, TW, PH1, and PH2). The matrix correlation explained little of the variation ($r = 0.250$) and was not statistically significant ($P > 0.05$) (data not shown).

Demographic history

The mismatch distributions of the populations were multimodal, with the exception of those for the PH1and PH2 populations, which were unimodal. The range of the distributions of the PH1 and PH2 populations was obviously smaller than that of the others. The mismatch distribution of our entire set

Table 2. Pairwise F_{ST} values (below the diagonal) and *Nm* values (above the diagonal) for the mitochondrial DNA control region among 16 sampling localities of *Siganus fuscescens*. [a]Abbreviations of localities are shown in Table 1; Negative F_{ST} values were set to zero Significance thresholds: $^{*}P < 0.05$; $^{**}P < 0.01$; $^{***}P < 0.001$. ¶ Significant *p*-value after Bonferroni correction ($\alpha = 0.05$)

Locality[a]	CB	SZ	KG	CJ	AM	OK	MY	IS	TW	PH1	PH2	VT	TH	SM	PA	SR
CB		∞	∞	∞	1.294	0.871	1.753	2.365	25.116	1.991	2.093	7.293	4.591	0.252	3.582	3.181
SZ	0.000		∞	∞	1.763	1.125	2.441	3.471	25.778	2.273	2.382	7.679	4.554	0.261	4.810	3.144
KG	0.000	0.000		∞	1.445	0.957	2.006	2.797	31.992	2.389	2.475	8.145	4.860	0.260	5.017	3.647
CJ	0.000	0.000	0.000		1.677	1.101	2.358	3.422	41.523	2.763	3.061	10.858	6.837	0.297	6.077	4.423
AM	0.279***¶	0.221***¶	0.257***¶	0.230***¶		111.940	41.567	7.319	2.214	1.130	1.218	2.756	2.104	0.372	1.436	1.285
OK	0.365***¶	0.308***¶	0.343***¶	0.312***¶	0.004		10.116	3.687	1.457	0.769	0.840	1.869	1.458	0.367	0.951	0.883
MY	0.222***¶	0.170***¶	0.200***¶	0.175***¶	0.012	0.047*		220.068	2.995	1.856	1.972	3.505	2.713	0.355	2.151	1.790
IS	0.175***¶	0.126***¶	0.152***¶	0.127***¶	0.064*	0.119***¶	0.002		4.172	3.008	3.114	4.533	3.580	0.319	3.001	2.476
TW	0.020	0.019	0.015	0.012	0.184***¶	0.255***¶	0.143***¶	0.107***¶		2.599	2.940	∞	36.227	0.401	5.609	4.143
PH1	0.201***¶	0.180***¶	0.173***¶	0.153***¶	0.307***¶	0.394***¶	0.212***¶	0.143***¶	0.161***¶		34.672	2.557	2.432	0.215	3.237	5.597
PH2	0.193***¶	0.173***¶	0.168***¶	0.140***¶	0.291***¶	0.373***¶	0.202***¶	0.138***¶	0.145***¶	0.014		3.043	3.547	0.247	3.324	8.639
VT	0.064**	0.061*¶	0.058**	0.044*	0.154***¶	0.211***¶	0.125***¶	0.099***¶	0.000	0.164***¶	0.141***¶		∞	0.556	4.593	4.304
TH	0.098***¶	0.099**¶	0.093**	0.068*	0.192***¶	0.255***¶	0.156***¶	0.123**¶	0.014	0.171***¶	0.124***¶	0.000		0.556	3.798	5.729
SM	0.665***¶	0.657***¶	0.658***¶	0.627***¶	0.573***¶	0.576***¶	0.585***¶	0.610***¶	0.555***¶	0.700***¶	0.669***¶	0.474***¶	0.474***¶		0.270	0.281
PA	0.122***¶	0.094*¶	0.091***¶	0.076***¶	0.258***¶	0.344***¶	0.189***¶	0.143**¶	0.082*	0.134***¶	0.131***¶	0.098**	0.116**	0.650***¶		4.360
SR	0.135***¶	0.137***¶	0.121***¶	0.102***¶	0.280***¶	0.361***¶	0.218***¶	0.168***¶	0.108***¶	0.082***¶	0.055*	0.104***¶	0.080*	0.640***¶	0.103***¶	

of samples was tri-modal, with three small modes (Fig. 6). The model of sudden expansion could not be rejected for any of the populations and pooled sample by using the raggedness index (Harpending, 1994) (Table 4). This goodness of fit test, however, can rarely cause rejection of the sudden expansion model, even though there is obvious deviation from expected distributions under the model (Schneider and Excoffier, 1999). It seems that only the PH1 and PH2 populations have undergone purely demographic expansion (Slatkin and Hudson, 1991). Since three clades were detected in *S. fuscescens*, mismatch distribution analysis was also performed for each observed clade. The mismatch distributions for the three clades were unimodal, fitted the expected distributions under the sudden expansion model well, and did not cause rejection of the model of sudden expansion with a non-significant Harpending's raggedness index ($P > 0.05$) (Fig. 6).

The results of Tajima's *D* and Fu's *Fs* neutrality tests were significantly negative in several populations and the pooled sample ($P < 0.05$) (Table 4). Fu's tests of the three clades were negative and highly significant ($P < 0.001$), which indicated population demographic expansion for each clade of the species (Fig. 6). The tau value (τ), which provides a rough estimate of when the rapid population expansion started, varied widely from 0.00 to 23.72. The population size before and after expansion, θ_0 and θ_1, also indicated a wide range of values from 0.00 to 11.08, and from 4.32 to 9999, respectively (Table 4). Similar to the magnitude of values of Fu's *Fs*, the demographic estimated parameters τ and θ were at similar levels in the three clades (Fig. 6). The τ values of clades A, B, and C in *S. fuscescens* were 3.219, 3.312, and 3.172, respectively. The estimated time of expansion was approximately 18,000–46,000 years ago.

Morphological study

Morphometric measurements of *S. fuscescens* were compared among the three clades defined by the above molecular analysis. The results of measurements are shown in Appendix 3. The principal component analysis (PCA) of morphometric characteristics was conducted on 82 specimens using 30 measurements. In the PCA of measurements, the first and second principal components (PC) accounted for 25.70% and 11.66% of the variance, respectively. PC1 was loaded on predorsal length, first dorsal spine length, second dorsal spine length, longest dorsal spine length, last dorsal spine length, longest dorsal ray length, longest pectoral fin length, first anal spine length, second anal spine length, longest anal spine length, longest anal ray length, middle caudal fin length, snout length, and orbit diameter. PC2 was loaded on head length, last anal spine length, caudal peduncle length, length of upper lobe of caudal fin, length of lower lobe of caudal fin, and upper jaw length. The PCA revealed only 37.36% of the total variance expressed in the first two principal components, these being taken for principal component scores. In the measurements, the results showed that individuals of the three clades overlapped completely (Fig. 2), indicating that no significant differences existed in the measurements for these genetically defined clades in the present genetic analyses. In addition, the plots of head length versus longest pectoral fin length for three clades also overlapped, and we could not separate them (Fig. 2).

Discussion

Our results indicated that no significant genetic structure was observed among populations around the main island of Japan (CB, SZ, and KG) and CJ, and these populations were genetically the same over a large geographical range, whereas most of the other populations examined in the present study

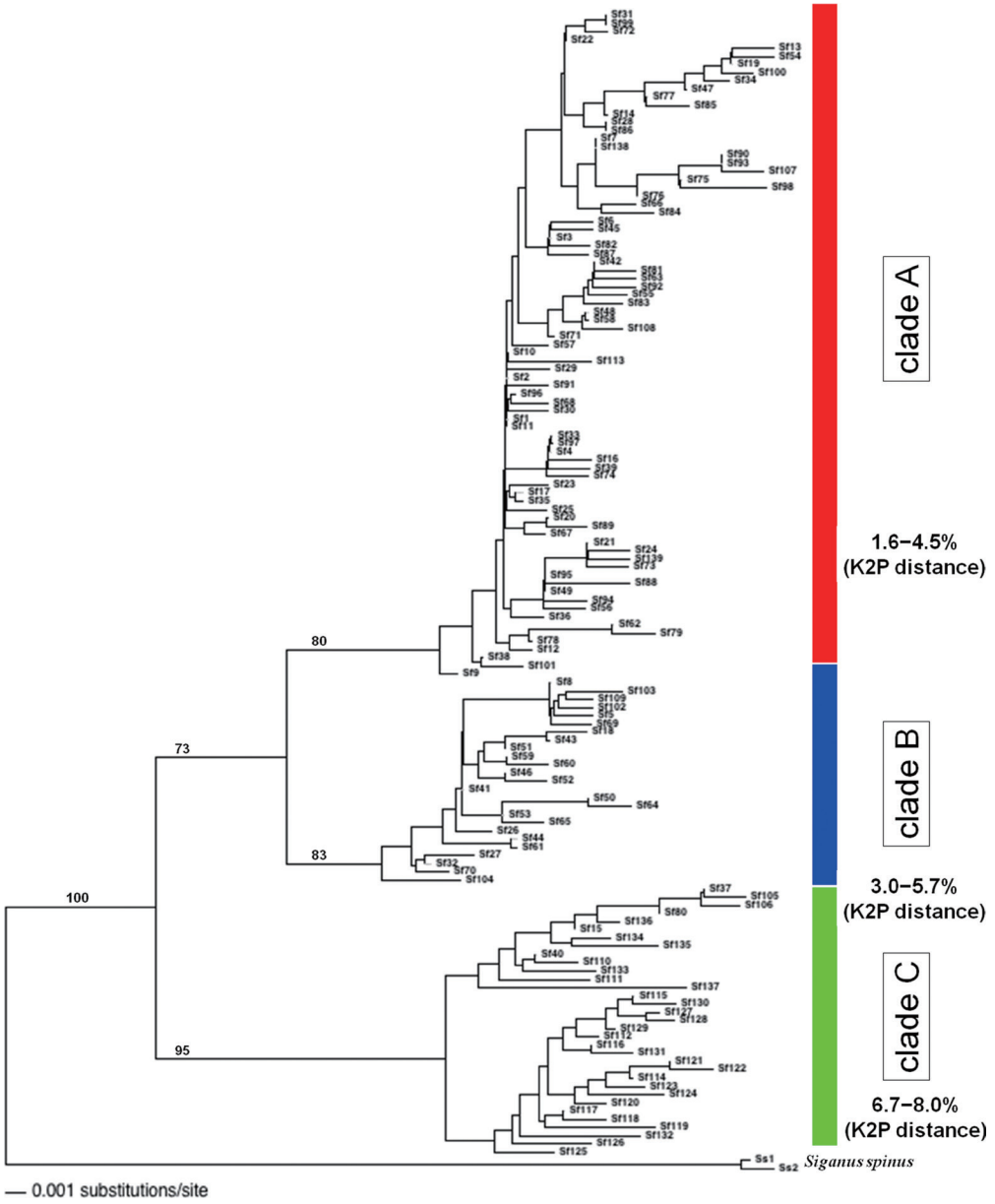

Fig. 4. Neighbor-joining tree based on genetic distances estimated from the partial mitochondrial segment (449 bp) containing the partial tRNAThr gene, entire 68-bp tRNAPro gene, and partial control region of *Siganus fuscescens*. Distance estimations based on Kimura's two-parameter model. Numbers above the major nodes indicate bootstrap support using the neighbor-joining method with equal weights for transitions and transversions based on 1,000 replicates. The congener, *S. spinus*, was used as an outgroup.

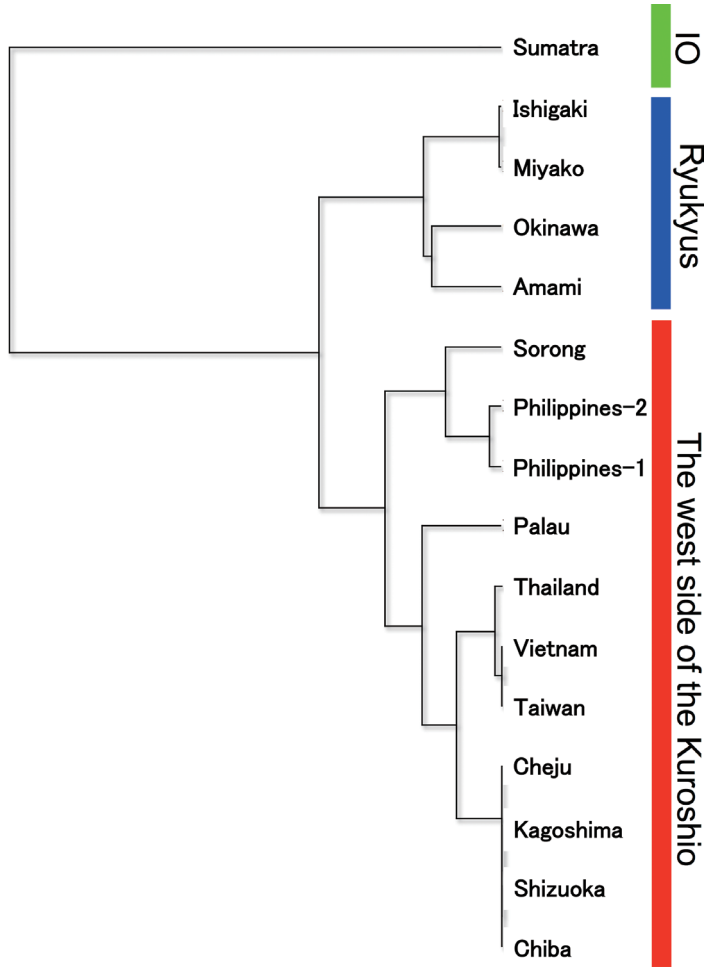

Fig. 5. Dendrograms of *Siganus fuscescens*. Constructed by the unweighted pair group method with arithmetic means (UPGMA) based on the pairwise F_{ST} values (Table 2). IO means the Indian Ocean.

Table 3. Summary of analysis of molecular variance (AMOVA) for mitochondrial DNA control region sequence of *Siganus fuscescens*. Abbreviations of localities are shown in Table 1; Significance thresholds: ***$P < 0.001$. *df*, degree of freedom; % var, percentage of variance Groups defined according to the pairwise F_{ST} (Table 3) and the dendrogram (Fig. 5).

Comparisons	Source of variance	*df*	% var	Fixation indices
All sites	Among populations	15	30.48	
	Within populations	69 9	69.52	F_{ST} = 0.312***
(CB, SZ, KG, CJ, TW, PH1, PH2, VT, TH, PA, SR), (AM, OK, MY, IS), (SM)	Among groups	2	39.20	F_{CT} = 0.392***
	Among populations	13	3.84	F_{SC} = 0.063***
	Within populations	69 9	56.97	F_{ST} = 0.430***

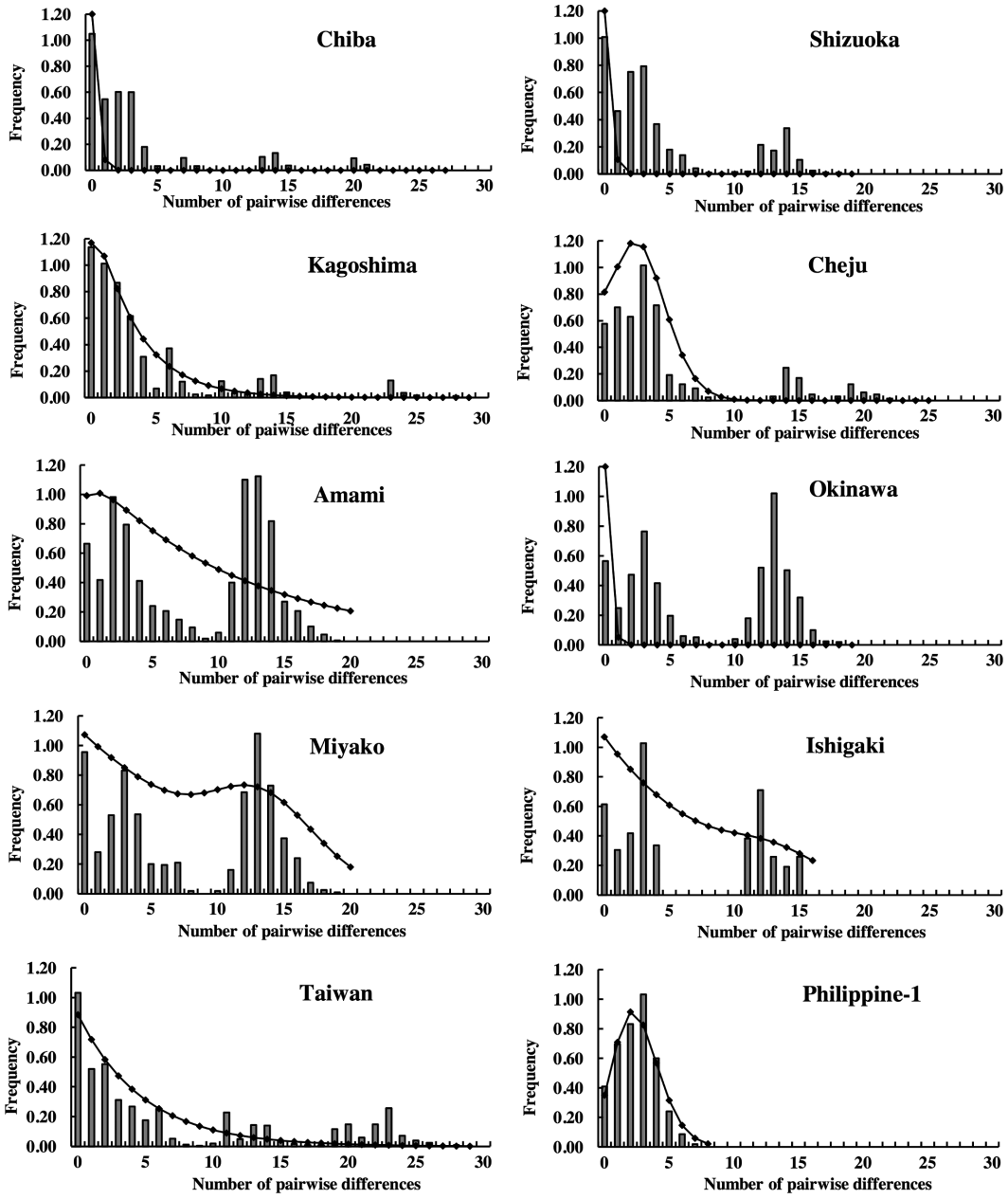

Fig. 6. Pairwise mismatch distributions for *Siganus fuscescens* by location, pooled samples and clades. The observed frequencies (bar) and the expected mismatch distributions under a model of sudden expansion (solid line) are shown for the mitochondrial DNA control region.

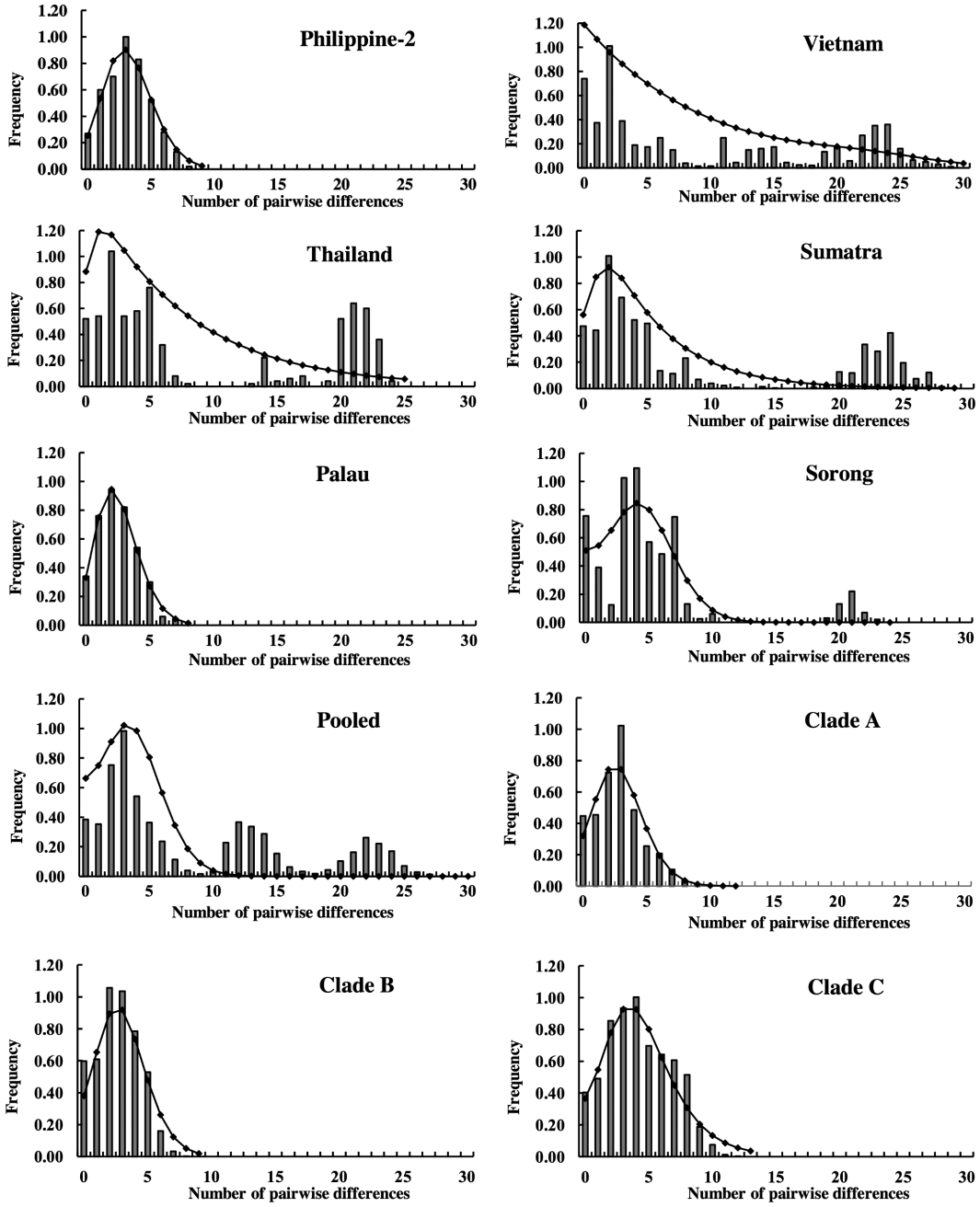

Fig. 6. Continued

were genetically distinct (Table 2). Most individuals from the CB, SZ, KG, and CJ populations belong to clade A. Paleo-climatic oscillations produced changes in temperatures and ocean current patterns, and displacement or eradication of coastal habitats (Bond *et al*. 1997; Kennett and Ingram, 1995; Kotilainen and Shackleton, 1995; Lambeck *et al*. 2002; Petit *et al*. 1999). In the study area, the northwestern Pacific region, shallow water habitats for coastal fishes including siganid species must have disappeared as the sea level declined in association with glaciation. The sea level was approximately 120 m lower than the present level during the glacial maxima (Bard *et al*. 1996; Rohling *et al*. 1998). Warm water fishes must have escaped to the south (to warmer areas), while some species stayed in habitats unsuitable for survival and faced extinction during glaciation resulting from atmospheric cooling. After glaciation, many species re-expanded or re-colonized northward.

Siganid fishes are considered to have originated in the central Indo-Malayan area (that is, a tropical area) (Woodland, 1990), and thus they are warm water fishes. Because the founder population, consisting of individuals belonging to the dominant genotypic group "clade A" in the study area (as identified using analysis of the mtDNA control region sequences), may have colonized and expanded to the northernmost distribution areas (CB, SZ, KG, and CJ) after glaciation, these populations will have the same genotype composition clustered on clade A. The pairwise F_{ST} and estimated *Nm* values of gene flow between the pairing of populations from CB, SZ, KG, and CJ indicate extremely high levels of gene flow and genetic homogeneities among these populations. The TW, VT, and TH populations were also genetically the same populations based on the calculated pairwise F_{ST} and estimated *Nm* values (Table 2), although sampled populations from TW, VT, and TH are more distant from each other. Geographically, the relationships among the CB, SZ, KG, and CJ populations are similar to those among the TW, VT, and TH populations, which means that sampling sites are relatively contiguous to each other along the coastal habitats. *Siganus fuscescens* inhabits coastal

Table 4. Results of the mismatch analysis and neutrality tests for *Siganus fuscescens*.

[a]Abbreviations of localities are shown in Table.1; corresponding *P*-values for each parameter are in parentheses.τ, expansion parameter; obs. mean, mismatch observed mean; θ_0, θ_1, mutation parameter before (θ_0) and after (θ_1) expansion. Ragged, raggedness index of Harpending (1994).

Locality[a]	parameter	Test of goodness of fit	Neutrality tests				
	τ	obs.	θ_0	θ_1	Ragged (*P*)	Tajima's *D* (*P*)	Fu's *Fs* (*P*)
CB	0.000	3.520	0.000	9999	0.039 (1.000)	-2.272 (0.000)	-3.336 (0.124)
SZ	0.000	4.32	0.000	9999	0.034 (1.000)	-1.632 (0.022)	-11.452 (0.002)
KG	0.414	4.072	2.693	6.194	0.018 (0.963)	-2.113 (0.005)	-7.677 (0.009)
CJ	3.453	4.775	0.007	7.994	0.027 (0.765)	-2.041 (0.004)	-4.502 (0.048)
AM	0.785	8.025	11.079	14.670	0.025 (0.469)	1.081 (0.891)	-1.521 (0.331)
OK	0.000	7.811	0.000	9999	0.038 (1.000)	1.041 (0.888)	-1.109 (0.394)
MY	14.484	7.769	0.000	12.348	0.031 (0.252)	1.031 (0.887)	-2.210 (0.228)
IS	14.330	6.268	0.000	8.256	0.079 (0.103)	1.049 (0.865)	1.249 (0.722)
TW	21.688	7.22	0.000	4.319	0.025 (0.888)	-1.099 (0.138)	-4.824 (0.077)
PH1	2.795	2.48	0.002	26.406	0.032 (0.579)	-1.144 (0.114)	-10.415 (0.000)
PH2	3.453	3.143	0.011	31.367	0.023 (0.760)	0.131 (0.612)	-3.981 (0.026)
VT	23.719	9.862	0.000	8.921	0.036 (0.373)	-0.235 (0.498)	-5.669 (0.063)
TH	0.611	9.444	7.044	50.803	0.026 (0.568)	-0.592 (0.311)	-2.466 (0.146)
SM	1.217	9.054	4.196	25.664	0.022 (0.492)	-0.824 (0.222)	-9.971 (0.005)
PA	2.523	2.474	0.072	59.062	0.029 (0.834)	-1.843 (0.012)	-8.083 (0.000)
SR	5.201	5.231	0.000	10.947	0.053 (0.135)	-1.063 (0.138)	-1.100 (0.383)
Pooled	4.395	8.7	0.000	9.318	0.015 (0.790)	-0.813 (0.254)	-23.872 (0.003)

waters, which may have permitted a very high level of gene flow over a large geographical distance due to the exchange of pelagic larvae along continuous shorelines.

In the Ryukyu Archipelago, although the sampling sites are located within 700 km of each other, restricted gene flow and genetic differentiation were observed (Table 2). Magsino and Juinio-Meñez (2008) investigated the influence of contrasting life history traits and oceanic processes on the population genetic structure of *S. fuscescens* and *S. argenteus* along the eastern Philippine coast using isozyme analysis. They have reported that populations of *S. fuscescens* were highly structured, whereas genetic structure was not observed between populations of *S. argenteus*. It is, however, still unclear how much distance they can be dispersed. The present results suggest that *S. fuscescens* will be able to cross less than the distance between Miyako and Ishigaki (*ca*. 120 km) in the oceanic environment by the transport of pelagic larvae, and there are several islands that may have worked as stepping-stones between Amami and Okinawa Archipelago. The gene flow between Okinawa and Miyako/Ishigaki islands seems to be restricted because of biological factors.

Based on the pairwise F_{ST} and Nm values and the UPGMA dendrogram, the Ryukyu Archipelago populations (AM, OK, MY, and IS) seem to be genetically isolated from other populations of the Kuroshio region. The hierarchical AMOVA test and the Mantel test supported the existence of this phenomenon. These results suggest that the boundaries between the Ryukyu Archipelago and Taiwan or the main island of Japan obviously exist and support the presence of barriers that prevent gene flow between them. The Kuroshio is a strong boundary current in the northwestern Pacific Ocean that begins off the Philippine islands, flows between the Ryukyu Archipelago and the island of Taiwan, and moves northeastward, dividing the Ryukyu Archipelago and the main island of Japan into parts. The biogeographical isolation of the Ryukyus is often explained by the distribution of the black seabream *Acanthopagrus schlegelii* and the Okinawa seabream *A. sivicolus*, which originated from a common ancestor (that is, they are sister species) (Hsu *et al*. 2011b). There are various documented reports on this kind of phenomenon occurring in not only fish species, but also mollusks and crustaceans (Aoki *et al*. 2008a; Aoki *et al*. 2008b; Imai and Aoki, 2012; Imai *et al*. 2013; Abdullah *et al*. 2014). Therefore, as a result of restricted gene flow between populations from the Ryukyu Archipelago and from Taiwan, the main island of Japan, or Cheju, the Ryukyu Archipelago populations are genetically isolated. On the other hand, although the island of Taiwan is more than 1,500 km from the main island of Japan and Cheju Island, genetic differentiation was not observed in the pairwise F_{ST} comparisons. This result suggests that there is a large distant gene flow among populations of these localities due to larval transport by the Kuroshio. Indeed, several studies have reported the northward transport of pelagic eggs and larvae by the Kuroshio for fish species (Tsukamoto, 1990; Sassa *et al*. 2006; Mukai *et al*. 2009). This indicates that the Kuroshio works for *S. fuscescens* not only as a strong barrier against their dispersal but also as a kind of conveyor for transporting, as proposed by Senou *et al*. (2006).

The MST and NJ tree of mtDNA control region haplotypes (Figs. 3 and 4) revealed that *S. fuscescens* is composed of three genetically divergent groups (clade A, clade B, clade C). Ravago-Gotanco *et al*. (2010) and Hsu *et al*. (2011a) have also revealed the presence of three genetic clades based on mtDNA control region and cytochrome *b* gene sequences. Although specimens were morphologically identified as *S. fuscescens*, in previous study, Ravago-Gotanco *et al*. (2010) regarded individuals of clade C as *S. canaliculatus*. All of the studies, including those by Ravago-Gotanco *et al*. (2010) and Hsu *et al*.

(2011a) referring to taxonomic issues, noted a lack of detailed morphological data that would allow one to make a distinction between *S. fuscescens* and *S. canaliculatus*. Most of these studies have distinguished *S. fuscescens* and *S. canaliculatus* based on color patterns (*i.e.*, spot density). Color pattern, however, is often an uncertain basis for taxonomy of fishes (Rocha, 2004), because of their color variations, especially in the case of some tropical fishes.

Our results using the PCA of 30 morphometric characteristics showed that morphological differences were not observed among the specimens of three genetically divergent groups. Plots of head length versus longest pectoral fin length for three clades overlapped (Fig. 2), also indicating this most common taxonomic key for distinction between *S. fuscescens* and *S. canaliculatus* was not sufficient for identifying them. The genetic distances of the mtDNA control region among three were 1.6–5.7% (K2P model), which were smaller than interspecific distance between *S. spinus* (K2P distance 6.7–8.0%) (Fig. 4). Kuriiwa *et al.* (2007) reported that the two morphotypes identified based on morphometric characteristics and color patterns constructed a genetic mosaic and were not reciprocally monophyletic for either nuclear DNA (ITS1) or mtDNA cytochrome b, suggesting that these are genetic color morphs within a single biological species. As a consequence of these results and reports, it should be appropriate that *S. fuscescens* and *S. canaliculatus* are considered a single biological species.

The present molecular analyses revealed three genetically distinct lineages, whereas the morphological analyses did not reveal such distinctions. The presence of divergence in the mtDNA and the absence of morphological divergence may be explained by the hypothesis that the three clades had once been isolated but are found in the same areas due to consequent secondary contact. In addition, three genetic clades were detected, but these clades did not appear to have clear geographic structure, which also might be the signature of admixture following past divisions. Because mtDNA is a non-recombinant and maternally inherited gene in at least fish species, genetic divergence formed during past isolation might be retained after secondary contact. Although the mismatch distribution analyses showed unimodal shapes for the PH1 and PH2 populations, the mismatch distributions for each population were multimodal profiles (Fig. 6), and each small mode corresponded to individuals within a clade comparison. The mismatch distribution of entire samples was trimodal, which suggests a conformation of the expectation of secondary contact and that data might include several genetically independent lineages.

The development of methods to test mutation drift equilibrium (MDE) allows tracing of the historical demography of a population from mtDNA data (Rogers and Harpending, 1992; Slatkin and Hudson, 1991). The frequency distribution of pairwise divergences between pairs of individuals, also known as mismatch distributions (Harpending *et al.* 1993), has been proposed as an alternative to sorting through phylogenetic trees to resolve the population history (Rogers, 1995). However, genetic discontinuities produced in isolation may generate mismatch distributions similar to those of a population at equilibrium (Marjoram and Donnelly, 1994). A spurious signal of this nature is of particular concern when studying the population history of widely distributed species. When there is evidence indicating secondary contact, it is appropriate to conduct MDE tests separately for each clade to avoid Type II errors resulting from the failure to reject a false null hypothesis of a population at equilibrium (Bowie *et al.* 2004; Gifford *et al.* 2004; Marmi *et al.* 2004; Michaux *et al.* 2004; Viñas *et al.* 2004). For these reasons, mismatch distributions and demographic history statistics for *S. fuscescens* were calculated for each clade.

For the three clades, the mismatch distributions

were unimodal, and they fit the expected distributions under the sudden expansion model well (Fig. 6). The calculated *Fs* results were negative and highly significant, which agreed well with the mismatch distribution analyses. These results indicate population demographic expansion for each clade of *S. fuscescens*, and the estimated time of expansion was approximately 18,000–46,000 years ago. According to the frequency of individuals of each clade for local populations (Fig. 1), clade A might have originated in the Coral Triangle, which is considered as an area of refuge from extinction by glaciation, and clade B might have originated around the Ryukyu Archipelago. Similar to this hypothesis of the origin of these clades, in previous study, Ravago-Gotanco *et al*. (2010) noted that clade B might have developed in the northwest Pacific, while clade C may be an Indian Ocean lineage. Kuriiwa *et al*. (2007) investigated genetically different lineages of the Indian-ocean specimens and regarded one group of specimens as an Indian Ocean type of *S. fuscescens*, as confirmed by Hsu *et al*. (2011a).

During interglacial periods and/or after the last glacial maxima (LGM), re-colonization might have resulted in demographic and spatial expansion. Our results suggest that population expansion occurred during the late Pleistocene in the three districts we studied. After that, the lineage of clade A might have colonized and expanded northward with the Kuroshio and along continuous shorelines. Clade B might have developed in the coastal areas along the paleo-Ryukyu Arc when the Kuroshio flowed eastward from the southern Ryukyu Archipelago due to the existence of a land bridge connecting the central-southern Ryukyu Archipelago to Taiwan during the last glacial stage (Ujiie *et al*. 1991; Ujiie *et al*. 1999; Ujiie *et al*. 2003). Following lineage development, this lineage might have been relatively isolated because of the course change of the Kuroshio axis to the modern current pattern after the LGM (Ujiie *et al*. 2003). For clade C, this kind of inter-oceanic differentiation between the Indian and Pacific oceans has been investigated in many coral reef fishes, such as the Daisy parrotfish, *Chlorurus sordidus* (Bay *et al*. 2004), three-spot dascyllus, *Dascyllus trimaculatus* (Bernardi *et al*. 2001; Leray *et al*. 2010), and false clownfish, Amphiprion ocellaris (Nelson *et al*. 2000). This separation of Indian Ocean and Pacific Ocean biotas and lineages coincides with a major marine biogeographic break referred to as the Sunda Shelf Barrier (reviewed by Carpenter *et al*. 2011). During sea level lows associated with glaciations, the increased isolation of the Indian and Pacific oceans may have promoted speciation. Such a scenario may account for the sibling species *S. fuscescens* and *S. canaliculatus*, the former a Pacific Ocean species and the latter an Indian Ocean species (Woodland, 1990). The dynamic change of land shapes may have influenced the speciation. Indeed, this pattern of Indian-Pacific Ocean speciation associated with the Sunda Shelf Barrier characterized by vicariant events resulting from Pleistocene sea level fluctuation has been reported in various marine species, such as butterflyfishes (McMillan and Palumbi, 1995; Timm *et al*. 2008) and anemonefishes (Timm *et al*. 2008). On the other hand, no phylogenetic structure across the Indo-West Pacific has been observed in marine fishes such as the soldierfish or surgeonfish species Craig *et al*. 2007; Klanten *et al*. 2007; Horne *et al*. 2008). Carpenter *et al*. (2011) concluded that these species lacking phylogenetic structure might have continued to successfully disperse during periods of glacial maxima, reestablished gene flow quickly after glacial maxima, lost divergent lineages, and undergone selective sweeps. In conclusion, the Sunda Shelf Barrier associated with Pleistocene fluctuations in the sea level might be not sufficient to explain why Indian-Pacific Ocean types of *S. fuscescens* speciated to two distinct species. Since our results indicated that most of the examined populations are composed

of the signatures of two or three formerly allopatric lineages, the sympatric occurrence of lineages might have resulted from secondary contact of genetically distinct lineages, which might have prevented speciation.

Another opinion is that the Indo-Pacific biogeographic border for fishes is not on the Sunda Shelf, but around the Cocos (Keeling) Islands and Christmas Island in the eastern Indian Ocean (Hobbs *et al*. 2009). At these islands, Indian and Pacific Oceans sibling species, at least six reef fish families (Hobbs *et al*. 2009), have come into contact and interbred. This suggests that a biogeographical border of Indo-Pacific species, including siganid species, may be located on the isolated islands in the eastern Indian Ocean. We examined individuals from the area along the east coast of Sumatra Island as Indian Ocean specimens. To understand their taxonomic status clearly and solve a taxonomic issue between *S. fuscescens* and *S. canaliculatus*, further research with specimens from the central and western Indian Ocean would have to be performed to examine the ecological as well as genetic aspects of the specimens.

Acknowledgements

We are grateful to Mr. Y. Yonamine of the Yaeyama Fisheries Cooperative Association, Mr. K. Kishiyama of the Shimizu Fisheries Cooperative Association, Mr. H. Ebihara of the Nishizaki Fisheries Cooperative Association, Dr. M. Imai and Mr. T. Shimomura of the Shizuoka Prefectural Government, Prof. V. Soliman of the Bicol University, Prof. Se-Jae Kim of the Jeju National University, Dr. Nguyen Khac Bat of the Research Institute for Marine Fisheries of Viet-Nam, Dr. K. Kuriiwa and Prof. A Takemura of University of the Ryukyus for their kind help in collecting specimens. We are also thanks to Mr. K. Miyamoto of the Okinawa Churashima Foundation for his help in depositing specimens. This study was partly supported by the Elucidation of "the Life History and Genetic Population Structure for Important Fisheries Fishes" from the Okinawa Prefectural Government, the Scientific Research Grant from the Saito Ho-on Kai and International Research Hub Project for Climate Change and Coral Reef / Island Dynamics.

References

Abdullah MF, Chow S, Sakai M, Cheng JH, Imai H. 2014. Genetic diversity and population structure of pronghorn spiny lobster *Panulirus penicillatus* in the Pacific region. *Pac. Sci*., **68**: 197-211.

Aoki M, Naruse T, Cheng JH, Suzuki Y, Imai H. 2008a. Low genetic variability in an endangered population of fiddler crab *Uca arcuata* on Okinawajima Island: analysis of mitochondrial DNA. *Fish. Sci*., **74**: 330-340.

Aoki M, Imai H, Naruse T, Ikeda Y. 2008b. Low genetic diversity of oval squid, *Sepioteuthis* cf. *lessoniana* (Cephalopoda: Loliginidae), in Japanese Waters inferred from a mitochondrial DNA non-cording region. *Pac. Sci*., **62**: 403-411.

Bard E, Hamelin B, Arnold M, Montaggioni L, Cabioch G, Faure G, Rougerie F. 1996. Deglacial sea-level record from Tahiti corals and the timing of global meltwater discharge. *Nature*, **382**: 241–244.

Bay LK, Choat JH, van Herwerden L. 2004. High genetic diversities and complex genetic structure in an Indo-Pacific tropical reef fish (*Chlorurus sordidus*): evidence of an unstable evolutionary past? *Mar. Biol*., **144**: 757–767.

Bernardi G, Holbrook SJ, Schmitt RJ. 2001. Gene flow at three spatial scales in a coral reef fish, the three-spot dascyllus, *Dascyllus trimaculatus*. *Mar. Biol*., **138**: 457–465.

Bond G, Shower W, Cheseby M, Lotti R, Almasi P,

DeMenocal P, Priore P, Cullen H, Hajdas I, Bonani G. 1997. A Pervasive Millennial-Scale Cycle in North Atlantic Holocene and Glacial Climates. *Science*, **278**: 1257–1266

Borsa P, Lemer S, Aurelle D. 2007. Patterns of lineage diversification in rabbitfishes. *Mol. Phylogenet. Evol.*, **44**: 427–435.

Bowie RCK, Fjeldså J, Hackett SJ, Crowe TM. 2004. Molecular evolution in space and through time: mtDNA phylogeography of the Olive Sunbird (*Nectarinia olivacea/obscura*) throughout continental Africa. *Mol. Phylogenet. Evol.*, **33**: 56–74.

Carpenter KE, Barber PH, Crandall ED, Ablan-Lagman MCA, Ambariyanto, Mahardika GN, Manjaji-Matsumoto BM, Juinio-Meñez MA, Santos MD, Starger CJ, Toha AHA. 2011. Comparative phylogeography of the coral triangle and implications for marine management. *J. Mar. Biol.*, **2011**: 1–14.

Craig MT, Eble JA, Robertson DR, Bowen BW. 2007. High genetic connectivity across the Indian and Pacific Oceans in the reef fish *Myripristis berndti* (Holocentridae). *Mar. Ecol. Prog. Seri.*, **334**: 245–254.

Excoffier L, Lischer H. 2010. Arlequin suite ver 3.5: a new series of programs to perform population genetics analyses under Linux and Windows. *Mol. Ecol. Resour.*, **10**: 564–567.

Excoffier L, Smouse PE, Quattro JM. 1992. Analysis of molecular variance inferred from metric distances among DNA haplotypes: application to human mitochondrial DNA restriction data. *Genetics*, **131**: 479-491.

Felsenstein J. 1985. Confidence limits on phylogenies: an approach using the bootstrap. *Evolution*, **39**: 783–791.

Felsenstein J. 2004. *PHYLIP (Phylogeny Inference Package) version 3.6*. Distributed by the author. Department of Genome Sciences, University of Washington, Seattle.

Fu YX. 1997. Statistical tests of neutrality of mutations against population growth, hitchhiking and background selection. *Genetics*, **147**: 915–925.

Fujita D. 2006. How herbivorous fishes have interacted with seaweeds and their beds. *Jpn. Soc. Fish. Engineer.*, **43**: 53–58. (in Japanese with English abstract)

Gifford ME, Powell R, Larson A, Gutberlet Jr. RL. 2004. Population structure and history of a phenotypically variable teiid lizard (*Ameiva chrysolaema*) from Hispaniola: influence of a geologically complex island. *Mol. Phylogenet. Evol.*, **32**: 735–748.

Harpending RC. 1994. Signature of ancient population growth in a low-resolution mitochondrial DNA mismatch distribution. *Hum. Biol.*, **66**: 591-600.

Harpending HC, Sherry ST, Rogers AR, Stoneking M. 1993. The genetic structure of ancient human populations. *Curr. Anthropol.*, **34**: 483–496.

Horne JB, van Herwerden L, Choat JH, Robertson DR. 2008. High population connectivity across the Indo-Pacific: congruent lack of phylogeographic structure in three reef fish congeners. *Mol. Phylogenet. Evol.*, **49**: 629–638.

Hasegawa M, Koizumi K, Konagaya T, Noda M. 2003. Grazing of herbivorous fish as a continuous factor of Isoyake off the coast of Hainan, Shizuoka prefecture. *Bull. Shizuoka Pref. Fish. Exp. Stn.*, **38**: 19–25. (in Japanese)

Hobbs JPA, Frisch AJ, Allen GR, van Herwerden L. 2009. Marine hybrid hotspot at Indo-Pacific biogeographic border. *Biol. Lett.* **5**: 258–261.

Hsu KC, Chen JP, Shao KT. 2007. Molecular phylogeny of *Chaetodon* (Teleostei: Chaetodontidae) in the Indo-West Pacific: Evolution in geminate species pairs and species groups. *Raffles Bull. Zool. Suppl.*, **14**: 77–86.

Hsu TH, Adiputra YT, Burridge CP, Gwo JC. 2011a.

Two spinefoot colour morphs: mottled spinefoot *Siganus fuscescens* and white-spotted spinefoot *Siganus canaliculatus* are synonyms. *J. Fish Biol*., **79**: 1350–1355.

Hsu TH, Guillén Madrid AG, Burridge CP, Cheng HY and Gwo JC. 2011b. Resolution of the *Acanthopagrus* black seabream complex based on mitochondrial and amplified fragment-length polymorphism analyses. *J. Fish Biol*., **79**: 1182-1192.

Imai H, Aoki M. 2012. Genetic diversity and genetic heterogeneity of bigfin reef squid "*Sepioteuthis lessoniana*" species complex in northwestern Pacific Ocean. In: Mahmut Caliskan (ed.), *Analysis of Genetic Variation in Animals*. InTech, Rijeka, pp.151-166

Imai H, Hamasaki K, Cheng JH, Numachi K. 2004. Identification of four mud crab species (genus *Scylla*) using ITS-1 and 16S rDNA markers. *Aquat. Living Resour.*, **17**: 31-34.

Imai H, Hanamura Y, Cheng JH. 2013. Genetic and morphological differentiation in the Sakura shrimp (*Sergia lucens*) between Japanese and Taiwanese populations. *Contrib. Zool*., **82**: 123-130.

Iwamoto K, Chang CW, Takemura A, Imai H. 2012. Genetically structured population and demographic history of the goldlined spinefoot *Siganus guttatus* in the northwestern Pacific. *Fish. Sci*., **78**: 249–257.

Kennett JP, Ingram BL. 1995. A 20,000-year record of ocean circulation and climate change from the Santa Barbara basin. *Nature*, **377**: 510–514.

Kimura M. 1980. A simple method for estimating evolutionary rates of base substitutions through comparative studies of nucleotide sequences. *J. Mol. Evol*., **16**: 111–120.

Klanten SE, Choat H, van Herwerden L. 2007. Extreme genetic diversity and temporal rather than spatial partitioning in a widely distributed coral reef. *Mar. Biol*., **150**: 659–670.

Kocher TD, Thomas WK, Meyer AE, Edwards SV, Paabo S, Villablanca FX, Wilson AC. 1989. Dynamics of mitochondrial DNA evolution in animals: Amplification and sequencing with conserved primers. *Proc. Nat. Acad. Sci. U. S. A*., **86**: 6196-6200.

Kotilainen AT, Shackleton NJ. 1995. Rapid climate variability in the North Pacific Ocean during the past 95,000 years. *Nature*, **377**: 323–326.

Kuriiwa K, Hanzawa N, Yoshino T, Kimura S, Nishida M. 2007. Phylogenetic relationship and natural hybridization in rabbitfishes (Teleostei: Siganidae) inferred from mitochondrial and nuclear DNA analyses. *Mol. Phylogenet. Evol*., **45**: 69–80.

Kuriiwa K, Chiba SN, Motomura H, Matsuura K. 2014. Phylogeography of Blacktip Grouper, *Epinephelus fasciatus* (Perciformes: Serranidae), and influence of the Kuroshio Current on cryptic lineages and genetic population structure. *Ichthyol. Res*., **61**: 361–374.

Lambeck K, Esat TM, Potter EK. 2002. Links between climate and sea levels for the past three million years. *Nature*, **419**: 199–206.

Leray M, Beldade R, Holbrook SJ, Schmitt RJ, Planes S, Bernardi G. 2010. Allopatric divergence and speciation in coral reef fish: the three-spot Dascyllus, *Dascyllus Trimaculatus*, species complex. *Evolution*, **64**: 1218-1230.

Magsino RM, Juinio-Meñez MA. 2008. The influence of contrasting life history traits and oceanic processes on genetic structuring of rabbitfish populations *Siganus argenteus* and *Siganus fuscescens* along the eastern Philippine coasts. *Mar. Biol*., **154**: 519–532.

Marjoram P, Donnelly P. 1994. Pairwise comparisons of mitochondrial DNA sequences in subdivided populations and implications for early human evolution. *Genetics*, **136**: 673–683.

Marmi J, Bertranpetit J, Terradas J, Takenaka O, Domingo-Roura X. 2004. Radiation and phylogeography in the Japanese macaque, *Macaca fuscata*.

Mol. Phylogenet. Evol., **30**: 676–685.

Michaux JR, Libois R, Paradis E, Filippucci MG. 2004. Phylogeographic history of the yellow-necked fieldmouse (*Apodemus flavicollis*) in Europe and in the near and Middle East. *Mol. Phylogenet. Evol*., **32**: 788–798.

McMillan WO, Palumbi SR. 1995. Concordant evolutionary patterns among Indo-West Pacific butterflyfishes. *Proc. R. Soc. Lond*., **260**: 229–236.

Meyer AE, Kocher TD, Basasibwaki P, Wilson AC. 1990. Monophyletic origin of Lake Victoria cichlid fishes suggested by mitochondrial DNA sequences. *Nature*, **347**: 550553.

Mukai T, Nakamura S, Nishida M. 2009. Genetic population structure of a reef goby, *Bathygobius cocosensis*, in the northwestern Pacific. *Ichthyol. Res*., **56**: 380–387.

Nei M. 1987. *Molecular Evolutionary Genetics*. Columbia University Press, New York, USA, p 180.

Nelson JS, Hoddell RJ, Chou LM, Chan WK, Phang VPE. 2000. Phylogeographic structure of false clownfish, *Amphiprion ocellaris*, explained by sea level changes on the Sunda shelf. *Mar. Biol*., **137**: 727–736.

Petit JR, Jouzel J, Raynaud D, Barkov NI, Barnola JM, Basile I, Bender M, Chappellaz J, Davis M, Delaygue G, Delmotte M, Kotlyakov VM, Legrand M, Lipenkov VY, Lorius C, Pepin L, Ritz C, Saltzman E, Stievenard M. 1999. Climate and atmospheric history of the past 420,000 years from the Vostok ice core, Antarctica. *Nature*, **399**: 429-436.

Ravago-Gotanco RG, Juinio-Menez MA. 2010. Phylogeography of the mottled spinefoot *Siganus fuscescens*: Pleistocene divergence and limited genetic connectivity across the Philippine archipelago. *Mol. Ecol*., **19**: 4520–4534.

Rice WR. 1989. Analyzing tables of statistical tests. *Evolution*, **43**: 223–225.

Rocha LA. 2004. Mitochondrial DNA and color pattern variation in three Western Atlantic *Halichoeres* (Labridae), with the revalidation of two species. *Copeia*, 2004: 770–782.

Roberts CM. 1997. Connectivity and management of Caribbean coral reefs. *Science*, **278**: 1454–1457.

Rogers AR. 1995. Genetic evidence for a Pleistocene population explosion. *Evolution*, **49**: 608–618.

Rogers AR, Harpending H. 1992. Population growth makes waves in the distribution of pairwise genetic differences. *Mol. Biol. Evol*., **9**: 552-569.

Rohling EJ, Fenton M, Jorissen FJ, Bertrand P, Ganssen G, Caulet JP. 1998. Magnitude of sea-level lowstands of the past 500,000 years. *Nature,* **394**: 162–165.

Saitou N, Nei M. 1987. The neighbor-joining method: a new method for reconstructing phylogenetic tree. *Mol. Biol. Evol*., **4**: 406–425.

Sassa C, Konishi Y, Mori K. 2006. Distribution of jack mackerel (*Trachurus japonicus*) larvae and juveniles in the East China Sea, with special reference to the larval transport by the Kuroshio Current. *Fish. Oceanogr.* **15**: 508–518.

Schneider S, Excoffier L. 1999. Estimation of past demographic parameters from the distribution of pairwise differences when mutation rates vary among sites: application to human mitochondrial DNA. *Genetics*, **152**: 1079–1089.

Senou H, Matsuura K, Shinohara G. 2006. Checklist of fishes in the Sagami Sea with Zoogeographical comments on shallow water fishes occurring along the coastlines under the influence of the Kuroshio Current. *Mem. Nat. Sci. Mus. Tokyo*, **41**: 389–542.

Shields GS, Kocher TD. 1991. Phylogenetic relationship of North American ursids based on analysis of mitochondrial DNA. *Evolution*, **45**: 218–221.

Shimada K. 2000. Family Siganidae. In: Nakabo T (ed) *Fishes of Japan with Pictorial Keys to the species, English edition*. Tokai University Press, Tokyo, pp. 998–1087.

Slatkin M, Hudson RR. 1991. Pairwise comparisons

of mitochondrial-DNA sequences in stable and exponentially growing populations. *Genetics*, **129**: 555-562.

Sokal RR, Michener CD. 1958. A statistical method for evaluating systematic relationships. *Univ. Kansas sci. Bull*., **38**: 1409–1438.

Soliman V, Bobiles RU, Yamaoka K. 2009. Overfishing in three siganid species (Family: Siganidae) in Lagonoy Gulf, Philippines. *Kuroshio Sci*., **2**: 145–150.

Swofford DL. 2002. *PAUP*: phylogenetic analysis using parsimony* (* and other methods). Version 4b10, Sinauer Associates, Sunderland, Massachusetts.

Tajima F. 1983. Evolutionary relationship of DNA sequences in finite populations. *Genetics*, **105**: 437460.

Tajima F. 1989. Statistical method for testing the neutral mutation hypothesis by DNA polymorphism. *Genetics*, **123**: 585-595.

Thompson JD, Gibson TJ, Plewniak F, Jeanmougin F, Higgins DG. 1997. The Clustal_X windows interface: flexible strategies for multiple sequence alignment aided by quality analysis tools. *Nucleic Acids Res*., **25**: 48764882.

Timm J, Figiel M, Kochzius M. 2008. Contrasting patterns in species boundaries and evolution of anemonefishes (Amphiprioninae, Pomacentridae) in the centre of marine biodiversity. *Mol. Phylogenet. Evol*., **46**: 268–276.

Tsukamoto K. 1990. Recruitment mechanism of the eel, *Anguilla japonica*, to the Japanese coast. *J. Fish Biol*., **36**: 659-671.

Ujiie H, Tanaka Y, Ono T. 1991. Late Quaternary paleoceanographic record from the middle Ryukyu Trench slope, northwest Pacific. *Mar. Micropaleontol*., **18**: 115–128.

Ujiie H, Ujiie Y. 1999. Late Quaternary course changes of the Kuroshio Current in the Ryukyu Arc region, northwestern Pacific Ocean. *Mar. Micropaleontol*., **37**: 23–40.

Ujiie Y, Ujiie H, Taira A, Nakamura T, Oguri K. 2003. Spatial and temporal variability of surface water in the Kuroshio source region, Pacific Ocean, over the past 21,000 years: evidence from planktonic foraminifera. *Mar. Micropaleontol*., **49**: 335–364.

Viñas J, Alvarado-Bremer JR, Pla C. 2004. Phylogeography of Atlantic bonito (*Sarda sarda*) in the northern Mediterranean: the combined effects of historical vicariance, population expansion, secondary invasion and isolation by distance. *Mol. Phylogenet. Evol*., **33**: 32–42.

Woodland DJ. 1990. Revision of the fish family Siganidae with descriptions of two new species and comments on distribution and biology. *Indo-Pacific Fishes* **19**: 1136.

Yamaoka K, Kita H, Taniguchi N. 1994. Genetic relationship in siganids from southern Japan. In: Proceeding of Fourth Indo-Pacific Fish Conference, Thailand, pp. 294–316.

(Received July 30, 2015; Accepted September 1, 2015)

Appendix 1. Summary of samples for morphological studies of *Siganus fuscescens*.

Locality	Clade	URM-P
CB	A	48546
	A	48547
	A	48548
	A	48549
	A	48550
	A	48551
SZ	A	48552
	A	48553
	A	48554
	A	48555
	A	48556
	A	48557
	A	48558
	B	48559
	A	48560
	B	48561
	A	48562
	A	48563
	A	48564
	A	48565
CJ	A	48566
	A	48567
	A	48568

Locality	Clade	URM-P
OK	B	46413
	B	46414
	A	46415
	B	46416
	A	46417
	B	46418
	A	46419
	B	46420
	A	46421
	A	46422
TW	A	44839
	B	44840
	B	44841
	B	44843
	C	44847
	A	44854
	A	44858
	C	44863
	B	44866
	C	44869
	C	44874
	A	44877
	A	44881
	C	44882
	A	44883

Locality	Clade	URM-P
PH1	A	48569
	A	48570
	A	48571
	A	48572
	A	48573
	A	48574
	A	48575
	A	48576
PH2	A	48577
	A	48578
	A	48579
	A	48580
	A	48581
	A	48582
	A	48583
	A	48584
	A	48585
VT	A	48586
	C	48587
	A	48588
	A	48589
	C	48590
	C	48591
	A	48592
	A	48593
	B	48594

Locality	Clade	URM-P
SM	C	48595
	A	48596
	B	48597
	A	48598
	C	48599
	C	48600
	C	48601
	C	48602
	C	48603

Appendix 2. Haplotype composition of 16 localities of *Siganus fuscescens*.

	CB	SZ	KG	CJ	AM	OK	MY	IS	TW	PH1	PH2	VT	TH	SM	PA	SR
Sf1	25	26	24	12	4	1	1	1	23			17	7	2	1	
Sf2	4	1	2	2												
Sf3	4	1	2	2	1	1	1	3		1	3					
Sf4	3	2	2	2					3			1	1			
Sf5	1	1	1	2												
Sf6	1	1	2	2												
Sf7	1	1	1	1		1	1	6	2	12	4	5	2	1		12
Sf8	1	1	1						1			1				
Sf9	1	1														
Sf10	1		2	2												
Sf11	1		2		1	2	1		1	1	2	1	1		6	1
Sf12	1															
Sf13	1															
Sf14	1															
Sf15	1								1			1	2			
Sf16		3	1	3												
Sf17		3	2	1								1				
Sf18		2														
Sf19		1	2	1	1	1	2		1			1		1		
Sf20		1	1													
Sf21		1		1												
Sf22		1		1												
Sf23		1		1												
Sf24		1														
Sf25		1										1				
Sf26		1														
Sf27		1														
Sf28		1														
Sf29		1														
Sf30		1														
Sf31		1														
Sf32			1													
Sf33			1													
Sf34			1													
Sf35			1													
Sf36			1													
Sf37			1						2			2				
Sf38			1	1					1							
Sf39				1												
Sf40				1					1			1				
Sf41					10	5	4	6	1			1		1		
Sf42					9	12	18	14		5	3					
Sf43					6	4	4									
Sf44					4	10	7	3								
Sf45					2	1	1									
Sf46					2	3	1									
Sf47					2		1									
Sf48					2		1			4	1					1
Sf49					2		3	2		3	3		1		1	
Sf50					1	5	2	3								
Sf51					1	1										
Sf52					1											
Sf53					1											
Sf54					1											
Sf55					1											
Sf56					1					1	1					
Sf57						1	1	3								
Sf58						1	1									
Sf59						1										
Sf60						1										
Sf61						1										
Sf62						1										
Sf63							1									
Sf64							1									
Sf65							1									
Sf66							1	1		1						
Sf67								2		3						
Sf68								1								
Sf69									1							
Sf70									1							
Sf71									1							
Sf72									1							
Sf73									1							
Sf74									1							
Sf75									1							
Sf76									1							
Sf77									1							
Sf78									1							
Sf79									1							
Sf80									1			2				
Sf81										2						
Sf82										2						
Sf83										1	2					
Sf84										1						**3**
Sf85										1						
Sf86										1						
Sf87										1						
Sf88										1						
Sf89										1						
Sf90											4	1	3	2		**11**
Sf91											3					
Sf92											2					
Sf93											1					
Sf94											1					
Sf95												1				
Sf96												1				
Sf97												1				
Sf98												1				
Sf99												1				
Sf100												1				
Sf101												1				
Sf102												1				
Sf103												1				
Sf104												1				
Sf53					1											
Sf54					1											
Sf55					1											
Sf56					1					1	1					
Sf57						1	1	3								
Sf58						1	1									
Sf59						1										
Sf60						1										
Sf61						1										
Sf62						1										
Sf63							1									
Sf64							1									
Sf65							1									
Sf66							1	1		1						
Sf67								2		3						
Sf68								1								
Sf69									1							
Sf70									1							
Sf71									1							
Sf72									1							
Sf73									1							
Sf74									1							
Sf75									1				1			
Sf76									1			1	1			
Sf77									1						1	**6**
Sf78									1				1			
Sf79									1							
Sf80									1			2				
Sf81										2						
Sf82										2						
Sf83										1	2					
Sf84										1						**3**
Sf85										1						
Sf86										1						
Sf87										1						
Sf88										1						
Sf89										1						
Sf90											4	1	3	2		**11**
Sf91											3					
Sf92											2					
Sf93											1					
Sf94											1					
Sf95												1				
Sf96												1				
Sf97												1				
Sf98												1				
Sf99												1				
Sf100												1				
Sf101												1				
Sf102												1				
Sf103												1				
Sf104												1				

Appendix 3. Morphometric characters of three genetic clades (A–C)[a] of *Siganus fuscescens*.

	clade A	clade B	clade C
Number of specimens	55	13	14
Standard length (mm)	90.7–261.1	110.3–282.5	114.3–226.6
In % of standard length			
body depth	34.9–42.7 (39.3)	37.5–41.1 (39.3)	36.8–42.3 (39.0)
head length	22.3–27.1 (24.6)	22.6–27.1 (25.4)	24.8–26.8 (25.5)
predorsal length	26.1–31.6 (28.8)	25.8–30.1 (28.1)	28.4–30.3 (29.2)
dorsal fin base length	67.7–73.9 (70.8)	69.6–73.3 (71.7)	69.7–71.8 (70.8)
first dorsal spine length	5.9–9.8 (8.2)	7.5–9.5 (8.5)	7.5–9.5 (8.6)
second dorsal spine length	9.2–12.7 (11.0)	10.1–12.9 (11.4)	8.8–13.5 (11.6)
longest dorsal spine length	9.9–15.3 (12.6)	10.5–14.4 (12.8)	12.4–15.1 (13.9)
last dorsal spine length	4.8–8.3 (6.4)	5.5–8.4 (6.7)	5.7–8.6 (7.5)
longest dorsal ray length	9.3–12.5 (11.1)	10.3–12.7 (11.5)	10.3–12.9 (11.7)
longest pectoral fin length	17.7–21.9 (19.7)	18.8–21.0 (20.3)	18.9–21.5 (20.2)
prepelvic length	30.5–35.0 (32.8)	31.4–34.3 (32.6)	31.9–34.1 (33.0)
longest pelvic fin length	12.3–14.8 (13.7)	12.5–14.9 (13.7)	13.4–15.3 (14.3)
preanal length	51.1–57.0 (54.1)	51.8–54.6 (53.7)	51.9–54.4 (52.8)
anal fin base length	39.2–46.8 (43.2)	42.2–45.0 (43.8)	43.0–46.0 (44.5)
first anal spine length	6.5–10.0 (8.4)	7.8–9.5 (8.8)	7.7–9.9 (8.7)
second anal spine length	9.8–13.0 (11.5)	10.2–12.9 (11.5)	11.5–13.0 (12.3)
longest anal spine length	9.0–13.8 (11.6)	10.6–12.8 (11.8)	11.6–14.0 (12.9)
last anal spine length	6.6–10.2 (8.7)	8.1–10.5 (9.1)	9.1–11.4 (10.2)
longest anal ray length	8.6–11.1 (9.8)	8.9–10.7 (9.8)	9.2–11.2 (10.4)
caudal peduncle length	8.4–11.6 (9.8)	8.3–10.6 (9.6)	9.5–11.0 (10.3)
caudal peduncle width	4.9–6.4 (5.8)	5.4–6.2 (5.8)	5.2–6.6 (6.0)
length of upper lobe of caudal fin	23.6–31.7 (27.5)	25.3–30.5 (28.1)	26.7–30.3 (28.7)
middle caudal fin length	15.3–20.2 (17.8)	16.5–18.5 (17.7)	17.2–20.3 (18.7)
length of lower lobe of caudal fin	20.4–30.0 (25.6)	23.0–27.4 (25.8)	25.1–27.8 (26.4)
In % of head length			
upper jaw length	24.0–29.4 (26.5)	23.4–26.7 (24.9)	24.1–27.7 (26.0)
snout length	37.6–46.1 (41.6)	37.6–44.0 (40.7)	37.3–42.2 (39.4)
orbit diameter	24.4–34.9 (29.3)	24.0–30.9 (27.5)	29.8–34.0 (31.8)
suborbital length	32.4–43.8 (37.6)	33.2–41.1 (36.7)	33.3–38.3 (35.5)
interorbital width	25.9–38.6 (32.0)	27.5–31.9 (29.7)	27.5–31.6 (29.6)

[a]Each group (clade A–C) was defined by molecular analysis.
Data include ranges, with means in parentheses